Selectively Compliant Underactuated Hand for Mobile Manipulation

Daniel Aukes*, Susan Kim†, Pablo Garcia†, Aaron Edsinger∞, and Mark R. Cutkosky*

Abstract— **The demands of mobile manipulation are leading to a new class of multi-fingered hands with a premium on being lightweight and robust as well as being able to grasp and perform basic manipulations with a wide range of objects. A promising approach to addressing these goals is to use compliant, underactuated hands with selectively lockable degrees of freedom. This paper presents the design of one such hand that combines series-elastic actuation and electrostatic braking at the joints. A numerical analysis shows how the maximum pull-out force varies as a function of kinematic parameters, spring forces at the joints and brake torques.**

I. Introduction

In the past decade there has been a renewed interest in underactuated robotic hands, a subject originally explored over 30 years ago [1] to allow secure grasping of a wide range of irregular objects without the cost, weight and complexity of fully actuated designs. Recent research has examined actuator control and placement in underactuated mechanisms [2][3]. Work has also addressed transmission design and analysis [4][5] and methods to allow some manipulation in an underactuated compliant design [6]. Other work has focused on adding small secondary motors to change the type of grasping and to expand the range of graspable objects [7].

The requirements of mobile manipulation particularly argue for underactuated, and back-driveable or series-elastic mechanisms[8][9][10]. These mechanisms allow hands to grasp a wide range of objects while remaining relatively simple, robust and lightweight. There is a premium on reducing mass at the end effector of a mobile robot, where additional weight has the greatest effect on both the robot and the environment, and where velocities are highest and impacts are most likely.

However, a typical disadvantage of underactuated designs is a loss in dexterity or grasp selection; underactuated hands are suited mainly for "power grasps" and not for manipulation with the fingers. There are a few exceptions. The SDM hand, for example is able to perform some manipulations at the fingertips by varying tension in the cables [11]. Another way to expand the repertoire is to add very small shape change actuators that actuate springs[7][12] to change the stiffness properties of the mechanisms. Adding a second actuator to a highly underactuated system has been shown to increase grasp stability [13].

Another strategy used to simplify the designs of hands is to employ non-backdriveable or locking mechanisms in the finger. Arai et al.[14] use joint locking in conjunction with the implicit dynamic coupling of series chains to actuate fingers. Takaki et al.[15] utilize a lightweight brake actuated by shape memory alloy to achieve high braking forces. The TWIX hand [16] utilizes a check valve to make the fingers non-backdriveable while allowing positive pressure to close the fingers. Several other designs utilize cam or clutch mechanisms to lock joints up to a certain torque threshold [17][18][19].

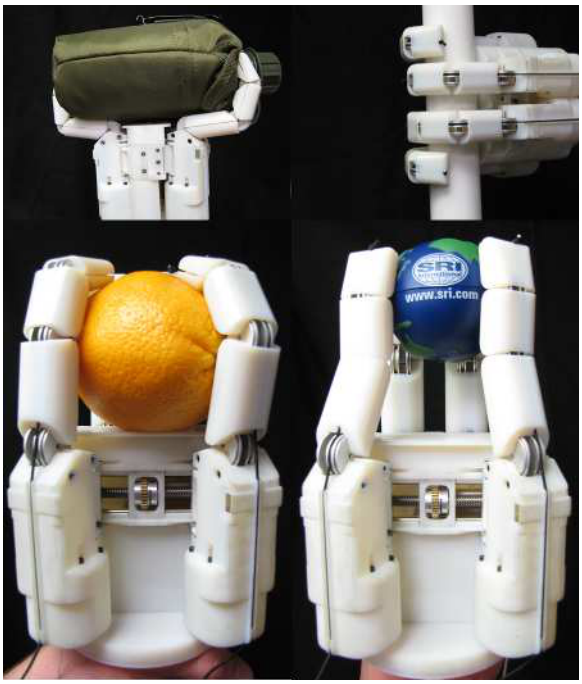

Fig. 1: The SRI Hand grasping a canteen, a pipe, an orange, and a small ball

This paper describes an underactuated hand design that allows locking and unlocking any of the finger joints using compact electrostatic brakes. The goal is to combine the simplicity and flexibility of underactuated hands for grasping irregular objects with the precision and deterministic behavior of fully actuated hands.

II. Design

A. Overview

The hand (Fig. 1) consists of four identical fingers each actuated by a modified version of a twisted string actuator [20]. Each finger has three phalanges connected in series with a cable running along pulleys in the joints, terminated at the fingertip. Since there are three independent degrees

This work was supported by DARPA and SRI International.

The authors are with: *the Department of Mechanical Engineering, Stanford University, Stanford, CA. † SRI International, Menlo Park, CA. ∞ Meka Robotics, San Francisco, CA.

D. Aukes danaukes@stanford.edu

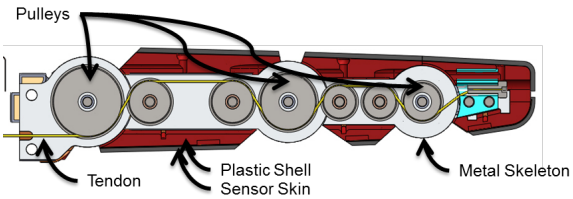

(a)

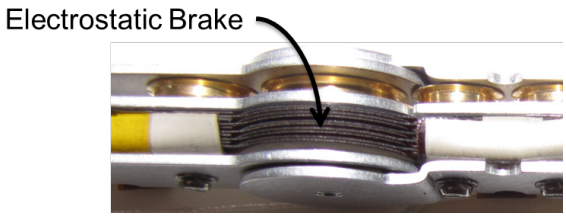

(b)

Fig. 2: (upper) Diagram of the finger showing pulleys and cable routing, (lower) photograph showing a side view of an electrostatic brake at a joint

of freedom in the finger and only one actuator, springs are attached across each joint to provide return actuation and to balance the closing tendon force between each phalanx. Extending from each phalanx into the joints is an interleaved set of surfaces used to electrostatically lock each joint [21]. Covering each phalanx is a set of capacitive force sensors similar to [22]. Tendon tension is measured using load cells integrated into the tendon path, allowing for force control using the tendon tension. The palm has one additional motor to enable reconfiguration of the finger positions and orientations, allowing for opposed, spherical, and interlaced grasps, as seen in the accompanying video [23].

B. Motivation for locking

The hand can hold a pose against arbitrarily large forces, up to the limits of the brakes. The drawback to such grasps is the potential for damage to the fingers once they are locked. Alternatively, one could have a hand that is back-driveable, and make sure the applied grasp forces exceed the forces that would pull the object out of the grasp. Looking at human hands, one gets the best of both worlds, because muscle can exert much larger forces when being "backdriven"[24].

1) Form Closure and Non-backdriveability: There are several factors influencing the choice to include brakes in each joint. First, by selectively unlocking a single joint at a time, we have full control over individual joint positions

variable	value	unit
$l_{link(i)}$	45, 30, 25	mm
$r_{pulley(i)}$	7.5, 6,5, 5	mm
$l_{spring0(i)}$	45, 30, 25	mm
$k_{spring(i)}$	50, 100, 135	N/m
f_{act}	10	N
$M_{brake(i)}$	0.5, 0.28, 0.13	N-m

TABLE I: Parameters used for Fingertip Analysis

Fig. 3: Joints 2 and 3 are locked and holding 1kg at the fingertip. (Joint 1 is against its joint limit)

within the limits of our braking torque and return spring force. Sequential joint operations give each finger full position control, allowing the finger to adopt any position within its workspace. This configuration space includes positions that are not in static equilibrium when underactuated. Being able to sequentially position the fingers in specific positions enables finger and grasp kinematics that would not be available with fully underactuated hands.

2) Motor Protection: Joint locking also allows us to reduce continuous motor current, lengthening the life of the motors and tendons. By locking finger joints we are able to maintain grasps without the motors drawing current and heating. The maximum time that motors have to remain on is the time required to obtain a certain grasp and engage the brakes.

III. Calculating Forces

A. Static Equations

Given that friction is uncertain, a suitable starting point for comparing the kinematic parameters, spring forces and brake torques of different designs is to assume zero friction when evaluating hands performing enveloping grasps. As mentioned in [25], calculating the quasi-static forces without friction means that the resulting configuration is not path-dependent, and is at the lowest potential energy. Finding the lowest energy state allows us to evaluate the differences between designs with different link lengths, etc. – as opposed to comparing different grasping strategies with and without friction – because the mapping between object position and resultant force can be one-to-one if the hand is properly

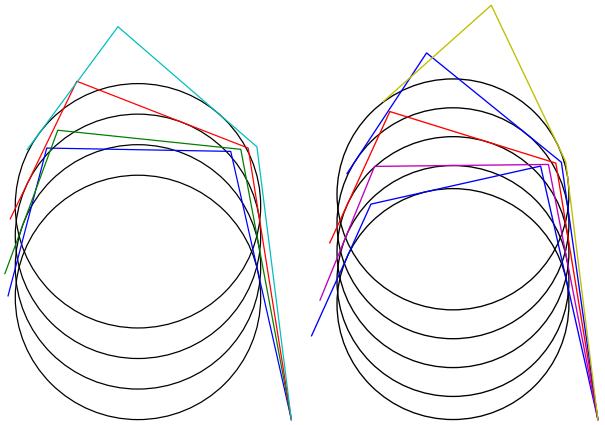

(a) (b)

Fig. 4: Two different grasp postures for an underactuated hand with locking capabilities. Figure (a) indicates the static equilibrium for the SRI hand. Phalanx 2 is not in contact with the circle at certain positions due to transmission and spring forces. With locking on, however (b), the fingers can be positioned to fully contact the same object, with reaction forces in the fingertips limited only by the limits of the joint brakes.

designed for the appropriate workspace. Of course, many grasps, including the pipe grasp in the upper right of Figure 1, require friction. Therefore, subsequent analysis should include friction to evaluate grasps.

We first define the Jacobians that map spring, actuator and contact normal forces to joint space. Finger parameters are supplied by table I, and the relationships between the rates of change for the tendon length, spring length, and velocity of the contact normals ($\dot{l}_{act}$, $\dot{l}_{spring}$, and $\dot{\mathbf{v}}_{cn}$, respectively) are described by

$$\dot{l}_{act} = \mathbf{J}_{act}\dot{\mathbf{q}}_j, \tag{1}$$

$$\dot{l}_{spring} = \mathbf{J}_s\dot{\mathbf{q}}_j, \tag{2}$$

$$\text{and } \dot{\mathbf{v}}_{cn} = \mathbf{J}_{cn}\dot{\mathbf{q}}_j. \tag{3}$$

The equations for static equilibrium can be derived using the principles of virtual work.

$$\dot{\mathbf{q}}_j^T \left(\mathbf{J}_{act}^T f_{act} + \mathbf{J}_{cn}^T \mathbf{f}_{cn} + \mathbf{J}_s^T f_s - \mathbf{M}_{brake}\right) = 0, \tag{4}$$

where f_{act} is the actuator force, $\mathbf{f}_{cn}$ is the vector of forces normal to contact, $\mathbf{f}_s$ is the vector of spring forces acting for each joint, and $\mathbf{M}_{brake}$ is the vector of reaction forces supplied by the locked joint brakes.

Normal contact forces are then calculated by setting $M_{brake} = 0$ in the unlocked case:

$$\mathbf{f}_{cn} = -\mathbf{J}_{cn}^{-T}\left(\mathbf{J}_{act}^T f_{act} + \mathbf{J}_s^T f_s\right). \tag{5}$$

The brakes are used to lock and unlock joints, so the analysis of break-away torque is a statics problem, where the resultant forces required must be evaluated against the maximum holding torque, supplied in table I. To estimate the resultant braking moment, M, let

$$\mathbf{M}_{brake} = \mathbf{J}_{act}^T f_{act} + \mathbf{J}_{cn}^T \mathbf{f}_{cn} + \mathbf{J}_s^T f_s \tag{6}$$

supplying a vector of intended contact forces at a given configuration of $\mathbf{q}_j = [q_1, q_2, q_3]^T$. In addition,

$$M_{brake(i)} = 2\tau\left(r_o^3 - r_i^3\right), \tag{7}$$

where r_o is the outer radius of the braking area, r_i is the inner radius of the braking area and τ is the effective shear stress applied in braking. Springs are assumed to behave linearly $k_{spring(i)}$ and are stretched to an initial value $l_{spring0(i)}$.

B. Equilibrium in Underactuated Fingers

Assuming that grasped objects are rigid and can withstand forces pushing normal to their surface, solving for the finger configuration that satisfies certain contact conditions is a kinematic problem. This can be accomplished by minimizing the distance between object and finger surfaces, using traditional minimization or optimization techniques, subject to certain constraints. One such constraint is that contact must occur within the length of each phalax.

$$\text{minimize} \sum_{i=1}^{3} \left|r(\mathbf{q})_{j(i)} - r_c\right|$$

$$\text{subject to } 0 \leq \frac{x_i}{l_i} \leq l_i, 1 \leq j \leq 3,$$

where $r(\mathbf{q})_{j(i)}$ is the calculated distance from phalanx i to the center of the circle as a function of the joint angles, r_c is the radius of the circle, x_i is the contact location along phalanx i, and l_i is the length of phalanx i. For example, Fig. 4b shows a series of grasps which kinematically solve for contact on a circlular object at different distances from the palm.

Solving for static equilibrium when grasping with an underactuated finger is not straightforward, however, because

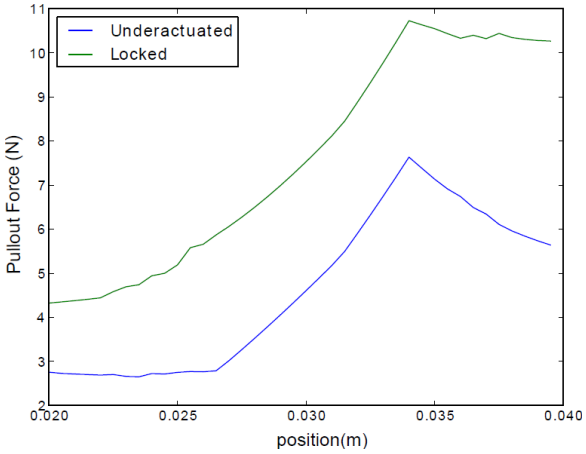

Fig. 5: Finger pullout forces on a circle as it is pulled in the y-direction for both a locked and unlocked finger with tendon tension at 10N. The x-axis indicates the position of the circle shown in fig 4a. The grasp becomes unstable at y=33mm

positive normal forces cannot be guaranteed in all configurations [5]. When a negative normal force is encountered in a particular contact, this corresponds to the associated phalanx losing contact. This forces us to consider contact forces at the phalanges that encounter such a loss of contact.

$$\begin{aligned}\text{minimize } & \sum_{i=1}^{3} \left| r(\mathbf{q})_{j(i)} - r_c \right| s_i \\ & + \sum_{i=1}^{3} \left(\left| r(\mathbf{q})_{j(i)} - r_c \right| - \left(r(\mathbf{q})_{j(i)} - r_c \right) \right) \bar{s}_i \\ & + \sum_{j=1}^{3} f_{cn(i)} \bar{s}_i \\ \text{subject to } & 0 \leq \frac{x_i}{l_i} \leq l_i, 1 \leq j \leq 3,\end{aligned}$$

where s_i is a boolean term that is true when normal forces are positive. Fig 4a shows a series of grasps which are solved for static equilibrium.

C. Equilibrium in partially locked fingers

The same method can be applied to fingers when one or two joints are locked. In this case the minimization algorithm is supplied with joint values for the locked joint(s) q_j and varies the remaining joint variables. With n=3 degrees of freedom and m=1 or 2 locked joints, the solver can generally find forces for n-m contact points without static indeterminacy. Soft finger models would be needed to calculate multiple points of contact in one locked phalanx.

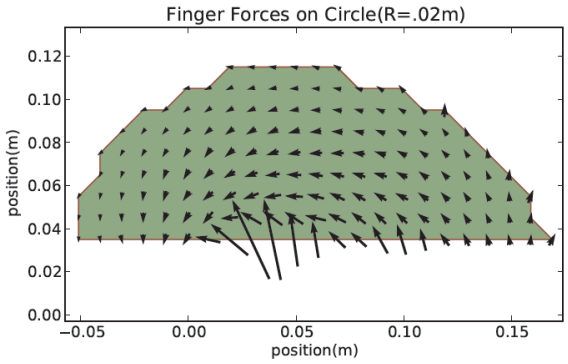

Fig. 7: Resultant forces on a circular object of R=0.02m for different positions within the finger's workspace. The finger is unlocked, its tension is 25N, and the maximum resultant force occurs at x = .03m, y = 0.035m, at 130N.

D. Equilibrium in fully locked fingers

In the case of fully locked fingers, any position can be considered to be in equilibrium, up to the maximum braking moments shown in table I. Fig 3 shows the finger moved to an arbitrary position and holding a 1kg load at the fingertips.

IV. Numerical Simulation

2-D Numerical simulation results have been obtained using WorkingModel 2005 for circular objects ranging from R=10mm to R=70mm. Objects are placed in a grid of positions evenly distributed throughout the finger's workspace, and resultant forces on the objects are calculated as the finger's tendon tension is increased from 0N to 150N(Fig 7). From these spatial data of the finger-object interaction,

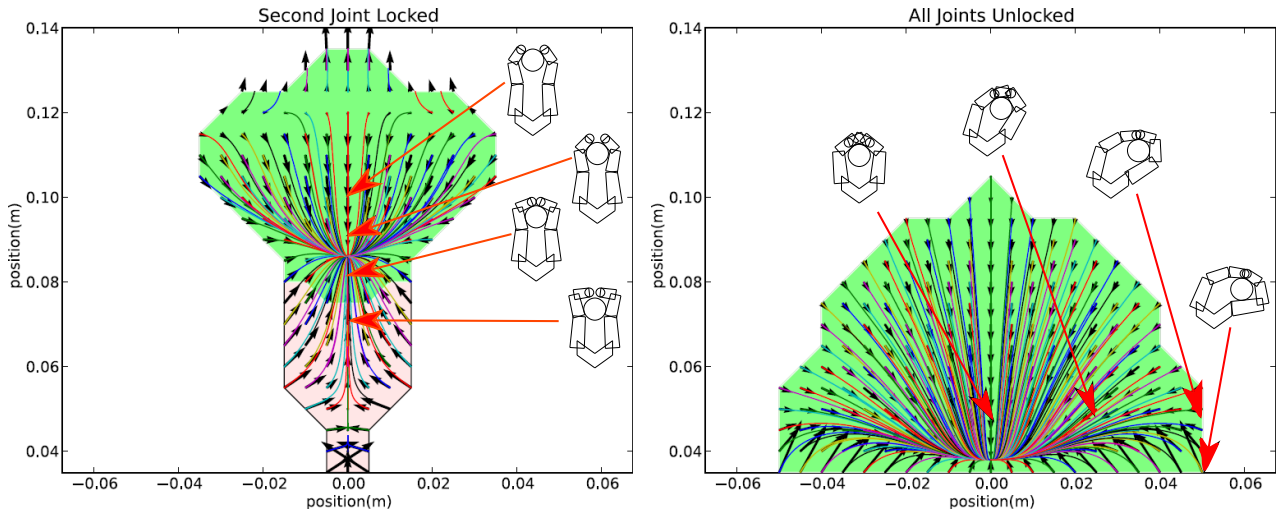

(a) (b)

Fig. 6: Two configurations of the hand grasping a circular object(R=.02m) with tendon tension = 25N. In (a), the second joint is locked, and the equilibrium loaction is located away from the palm. The darker green region indicates points where brake torques are within acceptable limits. The lighter red region indicates a region that is kinematically feasible but not possible due to brake slippage. In (b), none of the joints are locked and the equilibrium position is located at the palm. Since the joints are unlocked, we do not have to consider unacceptable brake torques.

regions can be calculated where objects are likely to be captured. The result is obtained by mirroring and superimposing force data across the y axis to create a set of forces for two fingers in an opposed grasp. By interpolating between the original data points, a system of first-order differential equations can be integrated numerically for starting points throughout the hand's workspace, allowing us to generate regions similar to the concept of stability cells discussed in [25]. External forces can also be added to the force field to evaluate grasping performance due to disturbances. To consider the effect of locked joints on the the object forces, joints are modeled in the simulation as stiff torsional springs (k = 100N-m / rad), that can be locked at any joint orientation. The simulation has been performed for a finger in two configurations. In the first configuration, the second phalanx is locked in its open position to accomplish a pinch grasp with the fingertips. In the second, the joints are unlocked. Fig 6 shows the difference between the two configurations, and illustrates the difference in stability between the two types of locking configurations.

V. Manipulation

A. Fully-Actuated Manipulation

One type of manipulation can be accomplished by treating the grasped object as the output link of a parallel linkage (assuming the contact points can be approximated as simple rotational joints). By preshaping and locking fingers to specific lengths before contact, the fingers can act as two sides of a four-bar linkage. In this way, the object translates and rotates along a known path as a function of finger rotation, as seen in Fig 8.

B. Underactuated Manipulation

Different kinds of underactuated manipulations are made possible by switching locking configurations. They rely on unlocking more joints than there are actuators, allowing kinematics of the transmission and the energy stored in return springs to move the finger-object system to a new static equilibrium. Fig 9a exhibits the type of grasp one could expect to achieve by unlocking different combinations of joints.

Using the simulation results from section IV, we see an example of how a second type of underactuated manipulation may be accomplished. Fig 6a shows that with the second joint locked and the two tendons exerting a force of 25N,

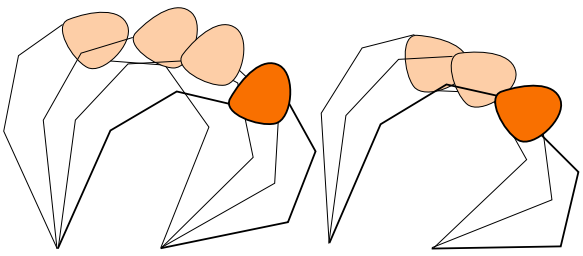

Fig. 8: Two different locked finger configurations create different motions in the grasped object, shown in orange.

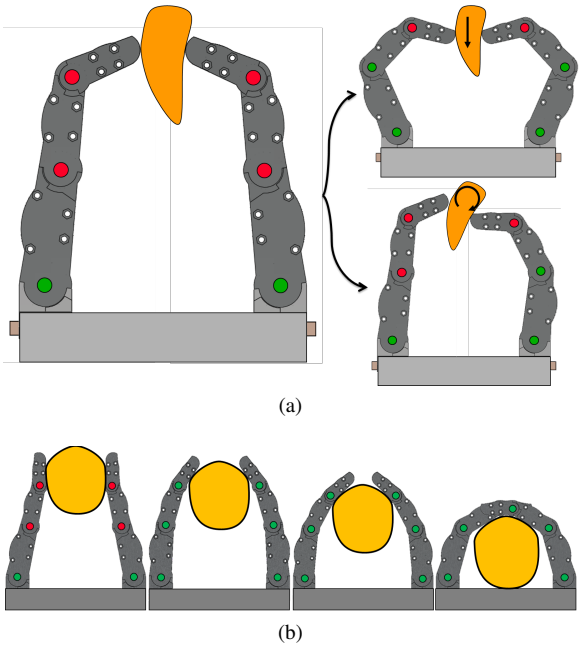

(a)

(b)

Fig. 9: By unlocking the joints in (a), the fingers can perform small manipulation moves, such as translation and rotation. Whole-hand manipulations, such as the pinch-to-wrap task shown in (b), can be attained by unlocking all the joints and allowing the fingers to wrap into their natural kinematics. The series of pictures illustrates how a pinched object, by slipping along the fingers, can move to a more stable grasp as the joints unlock. Locked joints are represented with a red dot, unlocked joints with a green dot

the resultant force on a circular object is in equilibrium when the object's center of mass is located at roughly .08m from the palm. In Fig 6b equilibrium occurs at the palm's surface. If the finger grasps an object in the first state and unlocks, the object will be drawn into a wrap grasp, as illustrated in 9b and demonstrated (despite some friction) in the accompanying video [23].

VI. Accompanying Video

As seen in the accompanying video [23], the SRI hand can adopt a range of poses by utilizing locking. It can be seen actuating individual joints, accomplishing a transition between pinch and wrap grasps, and turning on a grasped flashlight. In addition, the passive closing properties enable the hand to wrap around a wide variety of objects. At low tendon forces, the fingers are able to passively pinch small objects in the fingertips. At higher forces, they can securely grasp heavy objects and crush a soda can.

VII. Conclusions and Future Work

In this paper we have described an underactuated robotic hand that is able to conform to objects of various shapes and utilize selective locking to achieve grasps not otherwise possible with the given transmission and spring configuration. In addition, the selective locking allows the hand to perform certain manipulations of objects within the fingers.

Design work is continuing toward selecting kinematic and transmission characteristics that take best advantage of the locking capabilities. Initial results based on the analysis outlined in Section III and IV are yielding encouraging results.

There are still some design issues to be resolved with regard to electrostatic braking. Further research is required to find the desired tradeoff between electrical, mechanical, and geometric characteristics that will increase joint torque, improve locking speed, reduce wear, and improve durability. Even without optimization, however, this additional degree of configuration is already proving itself useful.

VIII. Acknowledgments

Support: Material herein is based upon work supported by the Defense Advanced Research Projects Agency (DARPA)/Defense Sciences Office (DSO) and Space and Naval Warfare System Center Pacific (SSC Pacific) under Contract No. N66001-10-C-4055.

Any opinions, findings and conclusions or recommendations expressed in this material are those of the author(s) and do not necessarily reflect the views of the agencies named above

References

[1] S. Hirose and Y. Umetani, "The development of soft gripper for the versatile robot hand," *Mechanism and Machine Theory*, vol. 13, pp. 351–359, Jan. 1978.

[2] L. Birglen and C. Gosselin, "Optimal design of 2-phalanx underactuated fingers," in *Proc. of IMG2004: IEEE international conference on Intelligent Manipulation and Grasping*, vol. pages, pp. 110–116, 2004.

[3] C. Gosselin and T. Laliberté, "Underactuated mechanical finger with return actuation," June 1998.

[4] T. Laliberté and C. Gosselin, "Actuation system for highly underactuated gripping mechanism," Jan. 2003.

[5] L. Birglen, C. Gosselin, and T. Laliberté, *Underactuated Robotic Hands*, vol. 40 of *Springer Tracts in Advanced Robotics*. Berlin, Heidelberg: Springer Berlin Heidelberg, 2008.

[6] R. Balasubramanian and A. M. Dollar, "Performance of serial underactuated mechanisms: Number of degrees of freedom and actuators," in *2011 IEEE/RSJ International Conference on Intelligent Robots and Systems*, pp. 1823–1829, IEEE, Sept. 2011.

[7] D. Aukes, B. Heyneman, V. Duchaine, and M. R. Cutkosky, "Varying spring preloads to select grasp strategies in an adaptive hand," in *2011 IEEE/RSJ International Conference on Intelligent Robots and Systems*, pp. 1373–1379, IEEE, Sept. 2011.

[8] J. B. Morrell and J. K. Salisbury, "Parallel-Coupled Micro-Macro Actuators," *The International Journal of Robotics Research*, vol. 17, pp. 773–791, July 1998.

[9] G. Pratt and M. Williamson, "Series elastic actuators," in *Proceedings 1995 IEEE/RSJ International Conference on Intelligent Robots and Systems. Human Robot Interaction and Cooperative Robots*, vol. 1, pp. 399–406, IEEE Comput. Soc. Press, 1995.

[10] A. Edsinger-Gonzales, "Design of a compliant and force sensing hand for a humanoid robot," in *Proceedings of the 2004 International Conference on Intelligent Manipulation and Grasping*, (Genova, Italy), pp. 291–295, DTIC Document, Citeseer, 2005.

[11] A. M. Dollar and R. D. Howe, "The Highly Adaptive SDM Hand: Design and Performance Evaluation," *The International Journal of Robotics Research*, vol. 29, pp. 585–597, Feb. 2010.

[12] J. Choi, S. Hong, W. Lee, S. Kang, and M. Kim, "A Robot Joint With Variable Stiffness Using Leaf Springs," *IEEE Transactions on Robotics*, vol. 27, pp. 229–238, Apr. 2011.

[13] L.-A. A. Demers and C. Gosselin, "Kinematic design of an ejection-free underactuated anthropomorphic finger," in *2009 IEEE International Conference on Robotics and Automation*, pp. 2086–2091, IEEE, May 2009.

[14] H. Arai and S. Tachi, "Position control of manipulator with passive joints using dynamic coupling," *IEEE Transactions on Robotics and Automation*, vol. 7, no. 4, pp. 528–534, 1991.

[15] T. Takaki and T. Omata, "100g-100N finger joint with load-sensitive continuously variable transmission," in *Proceedings 2006 IEEE International Conference on Robotics and Automation, 2006. ICRA 2006.*, no. May, pp. 976–981, IEEE, 2006.

[16] V. Begoc, S. Krut, E. Dombre, C. Durand, and F. Pierrot, "Mechanical design of a new pneumatically driven underactuated hand," in *Proceedings 2007 IEEE International Conference on Robotics and Automation*, no. April, (Roma), pp. 927–933, IEEE, Apr. 2007.

[17] M. Saliba and C. de Silva, "An innovative robotic gripper for grasping and handling research," in *Proceedings IECON '91: 1991 International Conference on Industrial Electronics, Control and Instrumentation*, pp. 975–979, IEEE, 1991.

[18] N. Ulrich, *Grasping with mechanical intelligence*. PhD thesis, School of Engineering and Applied Science, University of Pennsylvania, 1989.

[19] J.-u. Chu, D. Jung, and Y. Lee, "Design and control of a multifunction myoelectric hand with new adaptive grasping and self-locking mechanisms," in *2008 IEEE International Conference on Robotics and Automation*, pp. 743–748, IEEE, May 2008.

[20] T. Wurtz, C. May, B. Holz, C. Natale, G. Palli, and C. Melchiorri, "The twisted string actuation system: Modeling and control," in *2010 IEEE/ASME International Conference on Advanced Intelligent Mechatronics*, pp. 1215–1220, IEEE, July 2010.

[21] R. Kornbluh, R. Pelrine, H. Prahlad, and S. Stanford, "Mechanical Meta-Materials," Jan. 2006.

[22] J. Ulmen and M. Cutkosky, "A robust, low-cost and low-noise artificial skin for human-friendly robots," in *2010 IEEE International Conference on Robotics and Automation*, pp. 4836–4841, IEEE, May 2010.

[23] D. Aukes and S. Kim, "The SRI Hand (accompanying video)," 2012.

[24] F. E. Zajac, "Muscle and tendon: properties, models, scaling, and application to biomechanics and motor control.," *Critical reviews in biomedical engineering*, vol. 17, pp. 359–411, Jan. 1989.

[25] J. Trinkle, A. Farahat, and P. Stiller, "First-order stability cells of active multi-rigid-body systems," *IEEE Transactions on Robotics and Automation*, vol. 11, no. 4, pp. 545–557, 1995.